Metal-insulator transition in expanded alkali-metal fluids and alkali-metal—rare-gas films

Judy R. Franz

Department of Physics, Indiana University, Bloomington, Indiana 47405

(Received 5 May 1983; revised manuscript received 12 July 1983)

We have developed a theoretical model for expanded alkali metals and alkali-metal—rare-gas films that is based on a physically realistic picture of the atomic-scale structure of these materials. It emphasizes the disorder in the systems, in particular the random atomic coordination number. Using this model we have calculated the density- and the energy-dependent conductivity as a function of the mean alkali-metal atomic coordination number. Although the theory contains only two parameters, both of which are fixed by the properties of pure materials at normal temperatures, we have been able to explain results measured over a temprature range from 4.2 to >2000 K in a variety of different alkali-metal systems. Conductivity and magnetic-susceptibility measurements, in particular, have been considered in some detail. In addition, the theory provides insight into the nature and location of the metal-insulator transition, the nature of the critical point for the alkali metals, and the thermal instability of the alkali-metal—rare-gas films.

I. INTRODUCTION

Metal-insulator transitions have been studied with great interest recently, and a variety of theoretical models have been proposed to explain the experimental results in different materials.[1] The metal-insulator transitions in dilute alkali-metal systems such as expanded fluid alkali metals and alkali-metal—rare-gas films appear to be particularly favorable ones for testing theoretical models because of the relative simplicity of the systems. The expanded alkali metals seem particularly simple, having only one component and a half-filled s band. In these systems the transitions have been found to occur at densities near the liquid-gas critical point.[2,3] Unfortunately the experiments must thus be performed at extremely high temperatures and pressures so that interesting features of the transition may be smeared out. In contrast, experiments on alkali-metal—rare-gas films are carried out at very low temperatures, overcoming the problem of the expanded alkali metals, but now one must deal with a two-component system. In considering the results of these latter experiments, it has been common to consider the rare-gas atoms as inert spacers between the alkali-metal atoms. Although this is probably a good approximation, it is possible that small interactions between the alkali-metal electrons and the rare-gas atoms could affect the details of the metal-insulator transitions.

Among the mechanisms that have been proposed to explain the transitions in dilute alkali-metal systems are electron correlation effects leading to a Mott transition[4] and effects of disorder leading to Anderson localization.[5] Classical percolation theory has also been used to describe the transitions.[6] Because none of the calculations carried out so far have been able to describe all of the experimental measurements, it has also been proposed that more than one mechanism contributes to the observed effects.[3]

In the present paper we treat the effects of disorder in dilute alkali-metal systems. We show that a new type of Anderson transition may occur in these materials, one that is caused not by a randomness in the site energy levels or in the overlap integrals, as is usual, but by the randomness in the number of alkali-metal nearest neighbors, i.e, in the coordination number of the metallic component. It has been shown previously that this randomness can lead to the formation of localized states within the conduction band.[7-9] Most of these states lie at the center of the band and thus at the Fermi energy. The formation of these localized states is strongly coupled to the exclusion of extended states at the same energies, and both of these effects grow rapidly as the mean coordination number is reduced, i.e., as the alkali-metal systems become more dilute. Eventually a pseudogap forms in the alkali-metal band, causing a metal-nonmetal transition. These effects can be studied using the "quantum-percolation" Hamiltonian.[9-12]

The localization that occurs because of this quantum-percolation transition can explain the observed metal-insulator transitions in both expanded alkali metals and alkali-metal—rare-gas films, and appears to be sufficient to explain a wide variety of experimental measurements. The differences between the experimental results in the two types of materials are found to result almost entirely from the difference between the temperatures at which the experiments are performed. Moreover, the connection between the metal-insulator transitions and the critical points in the expanded alkalis can be understood within this model.

II. BACKGROUND

Classical percolation theory has been used by several experimental groups to explain their measurements of conductivity σ as a function of concentration in alkali-metal—rare-gas films.[6,13] Most percolation calculations have predicted the relationship

$$\sigma \propto (x - x_c)^s , \tag{1}$$

where x is the volume fraction of metal. Adler *et al.*[14] have argued that $s=2$, but different authors quote a range of values for the critical metal volume fraction, x_c. Phelps and Flynn[6] found that their measurements on Cs-Xe agreed well with Eq. (1) with $s=2$ and with the value of $x_c=0.15\pm0.01$ calculated by Scher and Zallen.[15] On the other hand, Swenumson *et al.*,[16] also working with Cs-Xe, found the best fit to their data with $s=3.3\pm0.1$ and $x_c=0.32\pm0.01$. Although the conductivity in these materials at low alkali-metal concentrations appears to resemble a percolation process, classical percolation theory does not allow one to calculate other important phenomena in these materials.

A recent calculation by Rose[4] investigated the effects of electron correlation in dilute alkali-metal systems as a function of uniform electron density. Using a spin-density-functional technique that did not include effects of disorder, Rose carried out a self-consistent band-structure calculation of the metal-insulator—transition density, magnetic susceptibility, and electron effective mass. He obtained a set of values for the alkali-metal critical radius parameters, $r_s^c=(3/4\pi n_c)^{1/3}$, where n_c is the critical number density, that are in qualitative agreement with experiments in both expanded alkali metals and alkali-metal—rare-gas films. Because zero temperature was assumed in the calculation, no distinction between high and low temperature could be made. Rose's calculation indicated that a first-order phase transition should occur in the alkali-metal—rare-gas films at a critical concentration. Because a smooth transition is observed experimentally, Rose suggested that the transition might be smeared by effects of disorder. In agreement with previous discussions of Mott transitions, Rose's calculation predicted a large magnetic susceptibility enhancement that should peak in the neighborhood of the metal-insulator transition and thus the critical density. A large magnetic susceptibility enhancement has been observed in expanded Cs; however, the peak in the enhancement appears to occur at twice the critical density, rather than at the critical density itself.[17] Rose suggested that this might also be caused by the effects of randomness. Because both these results, and previous model calculations that we had carried out, indicated that disorder in the arrangement of the atoms might be an important factor in the behavior of dilute alkali-metal systems, we decided to make a careful investigation of these effects.

The Anderson model for localization of electrons due to disorder[5] is usually discussed in a tight-binding framework. The original calculations included the effect of random atomic site energies, called diagonal disorder; other studies have incorporated randomness in the overlap (or hopping) integrals, called off-diagonal disorder. In the study of alloys a third type of disorder, the randomness in the type of nearest neighbors surrounding each atom, is important. This incorporates aspects of both diagonal and off-diagonal disorder. Jonson and Franz[8] investigated the random-alloy problem using a Monte Carlo method. They distinguished between localized and extended states using a method developed by Abou-Chacra *et al.*[18] and showed that localized states can persist at minority-band concentrations well above the classical percolation limit.

An important result of Jonson and Franz was the discovery that, for very large separation between the alloy-constituent atomic energy levels, a pseudogap persists in the center of the minority band over a wide concentration range. It is in this regime that the Anderson Hamiltonian reduces to the quantum-percolation Hamiltonian. Such localized states in the center of the band have also been reported by others.[7,9]

Expanded fluid alkali metals can be considered to be random alloys in which one component is entirely removed. Neutron-diffraction experiments on expanded rubidium[19] have shown that as the density of the fluid is decreased from that at the melting point to a value of about twice the critical-point density, the nearest-neighbor distance remains almost constant while the average number of nearest neighbors decreases. Thus the expansion of the alkali metals does not result in the distance between atoms increasing uniformly as has been assumed in a number of theoretical treatments, but to the development of an increasing number of vacancies. The important type of disorder in these materials therefore appears to be randomness in the number of nearest neighbors surrounding alkali-metal atoms. A model which simulates this important element of the real structure of these materials might thus be expected to predict observable effects that would be entirely lacking in the results of a calculation that assumes other types of disorder or expansion in an ordered system. This is indeed the case. As Jonson and Franz[8] showed, such a model predicts the existence of localized states lying within the energy band and thus of multiple mobility edges. It is the formation of a pseudogap in the center of the band, and thus for half-filled bands at the Fermi surface, which leads to the metal-insulator transition within this model.

The above model can thus be applied to both expanded alkali metals and alkali-metal—rare-gas films. The rare-gas atoms in the films are assumed to act as vacancies in the alkali-metal framework. An expectation of the model is, therefore, that the expanded alkali metals and alkali-metal—rare-gas films should behave similarly, with any differences being attributable to atomic size or temperature effects. As discussed below our results indicate that this is an accurate picture.

III. MODEL

We start by considering a random binary alloy described by the simple tight-binding Hamiltonian

$$H = \sum_i \epsilon_i n_i + \sum_{\substack{i,j \\ i \neq j}} t_{ij} c_j^\dagger c_i \ , \tag{2}$$

where i and j must be nearest neighbors for the hopping integral t_{ij} to be nonzero. In the alloy $A_x B_{1-x}$, the site energy ϵ_i can have one of two possible values ϵ_A or ϵ_B depending which type of atom occupies site i. The probability distribution for the random site energy is thus

$$P(\epsilon_i) = x\delta(\epsilon_i - \epsilon_A) + (1-x)\delta(\epsilon_i - \epsilon_B) \ . \tag{3}$$

This is the same model that was studied previously by Jonson and Franz,[8] which we will refer to henceforth as I.

To specialize this model to dilute alkali-metal systems, we let $|\epsilon_A - \epsilon_B|$ be large compared to the bandwidths of A and B and let $t_{AB} \rightarrow 0$. For expanded alkali metals, $t_{AB} = 0$, and there is only one band. Jonson and Franz[8] showed that for $t_{AB}/|\epsilon_A - \epsilon_B| \lesssim 10^{-3}$, the A and B bands are essentially noninteracting. For Cs-Xe this condition requires that $t_{AB}/t_{AA} \lesssim 0.05$, which seems quite reasonable for such a system. We thus focus our attention on the A band and take $t_{AA} = t$ and $\epsilon_i = \epsilon_A$.

We are interested in calculating the density of states and the conductivity. The magnetic susceptibility can then be estimated from the density of states (see Sec. V A). The density of states per atom, $g(\epsilon)$, is given by

$$g(\epsilon) = \pi^{-1} \langle A_{ii}(\epsilon) \rangle , \tag{4}$$

where

$$A_{ij}(\epsilon) \equiv -2 \operatorname{Im} G_{ij}(\epsilon + i\eta) \text{ as } \eta \rightarrow 0 , \tag{5}$$

so that A_{ii} is the diagonal component of the spectral density for the electronic Green's function, $G_{ij}(\epsilon + i\eta)$. The angular brackets are used to denote a configurational average over sites.

From the Kubo formula, the following exact expression for the dc conductivity $\sigma(0)$ in three dimensions can be derived using standard Green's-function techniques,

$$\sigma(0) = \frac{e^2 t^2}{6\pi\hbar\Omega} \int_{-\infty}^{\infty} d\epsilon \left[\frac{-dn_F(\epsilon)}{d\epsilon} \right]$$

$$\times \sum_{i,j} \sum_{\delta,\delta'} (-\vec{\delta} \cdot \vec{\delta}')$$

$$\times \langle A_{i,j+\delta'}(\epsilon) A_{j,i+\delta}(\epsilon) \rangle . \tag{6}$$

In this expression Ω is the volume of the system, $n_F(\epsilon)$ is the Fermi function, and $\vec{\delta} \equiv \vec{R}_{i+\delta} - \vec{R}_i$. When the electron mean free path is short, the position-space summation in Eq. (6) should converge rapidly. Thus for dilute systems the lowest-order term $\sigma_0(0)$ involving only two neighboring sites i and j should give a good approximation for the conductivity. This term is

$$\sigma_0(0) = \frac{\bar{Z} e^2 t^2 \delta^2 N}{6\pi\hbar\Omega} \int_{-\infty}^{\infty} d\epsilon \left[-\frac{dn_F(\epsilon)}{d\epsilon} \right]$$

$$\times \langle [A_{ii}(\epsilon) A_{jj}(\epsilon) - A_{ij}(\epsilon) A_{ij}(\epsilon)] \rangle , \tag{7}$$

where N is the number of conducting sites, $N/\Omega = \delta^{-3}$ is the density of these sites, and $\bar{Z}$ is the average coordination number for conducting sites. We can define an energy-dependent conductivity $\sigma_0(\epsilon)$ by

$$\sigma_0(0) = \int_{-\infty}^{\infty} d\epsilon \left[-\frac{dn_F(\epsilon)}{d\epsilon} \right] \sigma_0(\epsilon) . \tag{8}$$

Although Eq. (7) explicitly involves only two sites, the spectral-density function depends on the energies of all

sites. The two-site conductivity $\sigma_0(0)$ thus contains complete information about localization. We have used Eq. (7) to calculate conductivities in the work presented here.

In order to evaluate the density of states and the conductivity, it is necessary to evaluate the spectral-density function and thus the Green's function. The diagonal Green's function G_{ii} can be written in terms of the self-energy σ_i^t which describes hops away from site i,

$$G_{ii} = (\epsilon - \epsilon_A - \sigma_i^t)^{-1} . \tag{9}$$

It is possible to write the self-energy as a sum of terms, each corresponding to a nonrepeating path.[20] Keeping only the first term in this series, called the Cayley-tree approximation, greatly simplifies calculations. Although the Cayley-tree approximation gives a very poor description of good conductors, it has been found to give a relatively good description of systems in the strong scattering limit.[21,22] The Cayley-tree approximation is also expected to yield more accurate results as the coordination member decreases, becoming exact when $Z = 2$. For the dilute alloy systems, therefore, we expect it to give results that improve as the alkali-metal density is decreased.

Within the Cayley-tree approximation, the self-energy can be written

$$\sigma_i^t(\epsilon) = \sum_{k=1}^{Z} \frac{t^2}{\epsilon - \epsilon_A - \sigma_{i+k}(\epsilon)} , \tag{10}$$

where $\sigma_j(\epsilon)$, which describes forward hops from site j, is given by

$$\sigma_j(\epsilon) = \sum_{k=1}^{K} \frac{t^2}{\epsilon - \epsilon_A - \sigma_{j+k}(\epsilon)} . \tag{11}$$

Here K is the connectivity of the Cayley tree and is given by $K = Z - 1$. Equation (10) gives a recursion relation that allows the self-energies of individual sites to be calculated self-consistently. The Monte Carlo method used to determine an ensemble of independent self-energies has been described in I. In all of the calculations, checks were made to ensure that the results obatined were not dependent on either the size of the ensemble or the number of iterations. In most cases values of 100—200 were sufficient for both of these. In regions of rapid change typical values for the ensemble size and the number of iterations were 400 although occasionally larger values were used. Regions in which the scatter in the results remained significant are indicated with error bars on the graphs. For each of the self-energies, the components of the Green's function were calculated from Eq. (9) and from

$$G_{ij}(\epsilon) = G_{ii}(\epsilon) t / [\epsilon - \epsilon_A - \sigma_j(\epsilon)] . \tag{12}$$

From these the spectral-density functions and their appropriate ensemble averages can be calculated.

A principal difference between the calculations reported in I and the present ones is that here we are considering a one-component system. Thus each of the neighboring K sites either is occupied by an A atom or is taken to be vacant. For the expanded alkali metals the probability that the site is occupied is proportional to the density of the sample (see Sec. IV), while for the alkali-metal—rare-gas films it is given by the concentration of the alkali metals.

In both cases, the occupation of a particular site is chosen randomly so that the sum in Eq. (10) may contain from 0 to K nonzero terms. As the system becomes more dilute there are more sites with only a very small number of neighbors. The special localized states in the center of the band become important in the regime where the number of sites with only one nearest neighbor becomes non-negligible.[23]

As discussed by Abou-Chacra et al.[18] and by Jonson and Girvin,[24] the energy regions where electron states are localized can be determined by the condition that the probability that $\mathrm{Im}\sigma_i(\epsilon+i\eta)$ equals zero tends to unity as $\eta \rightarrow 0$. In practice the ensemble average of $\mathrm{Im}\sigma_i(\epsilon)$ in the localized regime can be made arbitrarily small by increasing the number of iterations of Eq. (11) as described in I. Under these conditions the ensemble average of the spectral-density function tends to zero, which also causes the density of (extended) states [Eq. (4)] and the conductivity [Eq. (7)] to go to zero.

It should be noted that for certain alkali-metal densities, we find "localized" and extended states coexisting at the same energy. This coexistence of localized and extended states has been reported by others,[7,9,12] and is possible because extended states are excluded from regions of space where localized states exist. There are a small number of localized states due to isolated clusters scattered throughout the band. The effect of these states is negligible, however, because the probability of even small clusters is very low in the concentration region of interest. As we will show in Sec. IV, in the center of the band, where most of the localized states are found, the extended states are gradually excluded as the concentration is lowered and the number of localized states grows. For $x \lesssim 0.2$, only localized states exist in the center of the band.

IV. NUMERICAL RESULTS

The model described above relates both the density of the expanded alkali metals and the alkali-metal concentration in alkali-metal—rare-gas flims to the mean alkali-metal coordination number $\bar{Z}$ of the atoms. The local atomic coordination number, on the other hand, is determined probabilistically and can vary from zero to Z_{max}. We define an effective alkali-metal concentration x_e by $x_e = \bar{Z}/Z_{max}$. Then for a fixed Z_{max}, x_e is proportional to the mean coordination number. For the alkali-metal—rare-gas films, x_e is equal to the actual alkali-metal concentration. An expanded alkali metal can be thought of as an alloy of alkali-metal atoms and vacancies. x_e is then the concentration of alkali-metal atoms in such a model. Evidence that such a description gives a good physical picture of the expanded alkali metals comes from neutron-diffraction measurements on expanded rubidium[3,20] taken along the liquid-vapor equilibrium curve. These results show that over a wide range of density (from the melting point almost to the critical point), the density is directly proportional to the coordination number while the nearest-neighbor distance changes by only a few percent. The density ρ of the fluid at any point can then be related to x_e by $\rho = x_e \rho_m$, where ρ_m is the density at the melting point.

An important aspect of describing both the high- and low-temperature systems with the same simple model is that only two parameters, Z_{max} and t, the hopping integral, are required for a complete description of both sets of systems. Both of these parameters can be determined from known properties of the alkali metals, so there are no adjustable parameters in the results reported in this paper. Most of the calculations described in this paper were carried out with $Z_{max} = 9$ since the rubidium neutron-
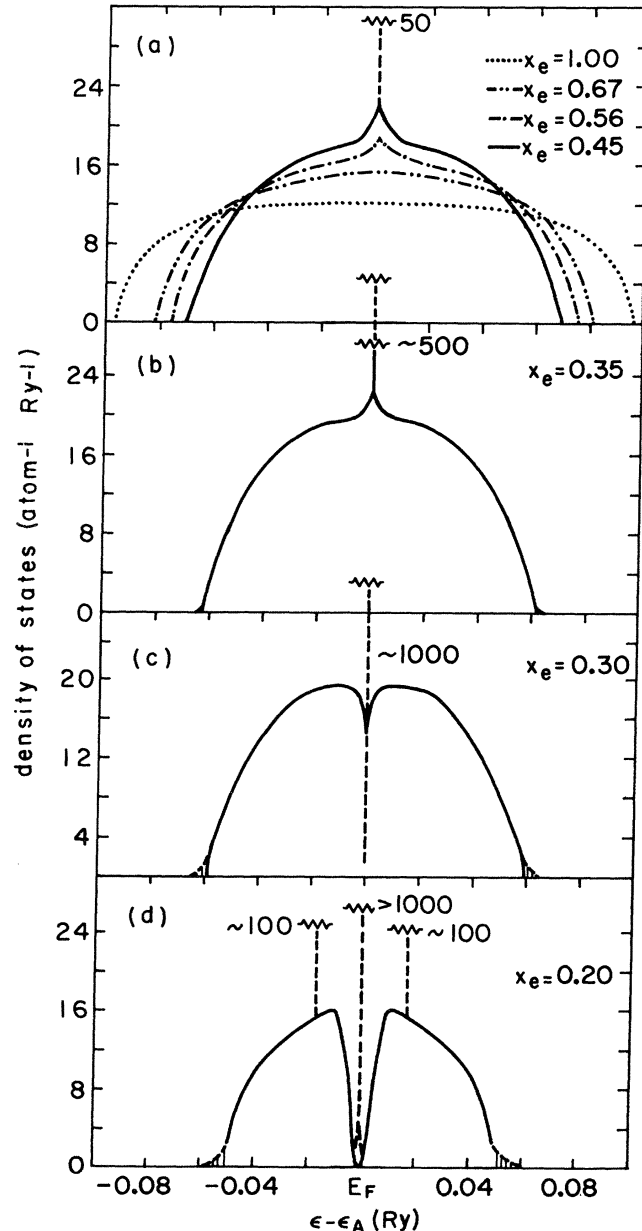

FIG. 1. Density of states per atom as a function of energy for various effective alkali-metal atomic concentrations x_e. Dashed lines in the center and at the edges (for $x_e \leq 0.35$) of the band indicate regions of localized states. For $x_e > 0.35$ the localized band tails are too small to be visible. Numbers near the sharp peaks indicate the approximate height of these peaks. (a) $x_e = 1.00$, 0.67, 0.56, and 0.45; (b) $x_e = 0.35$; (c) $x_e = 0.30$; (d) $x_e = 0.20$.

diffraction[3,20] results show that the coordination number near the melting point is close to this value. The results presented here are rather insensitive to the second parameter t which sets the absolute energy scale and is fixed by the alkali-metal bandwidth w ($w = 2Zt$ in the tight-binding model). A value $t = 0.017$ Ry was derived from the value of the Fermi energy for Cs and was used throughout this paper. For other alkali metals, higher values would be needed as discussed in Sec. V B.

The density of states per atom is shown as a function of energy in Fig. 1 for values of x_e ranging from 1.0 to 0.2 (for expanded alkali metals this corresponds to densities from ρ_m to values slightly below the critical density). The Fermi energy in each case is in the center of the band at $\epsilon = \epsilon_A$. Regions of localized states are shown by dashed lines. Several trends can be noted. As x_e, and thus the mean coordination number, is decreased starting from $x_e = 1.0$, the density of states per atom at the Fermi energy, $g(E_F)$/atom, at first increases because the band narrows with decreasing $\bar{Z}$ while the total number of states per atom is a constant. [$g(E_F)$/volume does not increase, however, because the density of alkali-metal atoms is decreasing. This will be discussed in Sec. V A.] At about $x = 0.60$, the density of states begins to peak up near the center of the band, i.e., near the Fermi energy. As x_e is decreased further this peaking becomes more pronounced until at $x_e \cong 0.45$, a very narrow spike of localized states occurs at the center of the band. It is as if states in the center of the band go through a percolation transition before states at other energies.[23] As expected, states in the band tails also become localized. With further decrease in x_e, the number of localized states grows rapidly. At $x_e \cong 0.30$, where the mean coordination number is ~ 3, all the extended states at the center of the band have disappeared, and a pseudogap opens up in the density of extended states. By $x_e = 0.20$, the density of extended states has shrunk appreciably, the pseudogap is very broad, and localized states appear not only at the center of the band but also at $\epsilon = \epsilon_A \pm t$, energies associated with electrons lo-
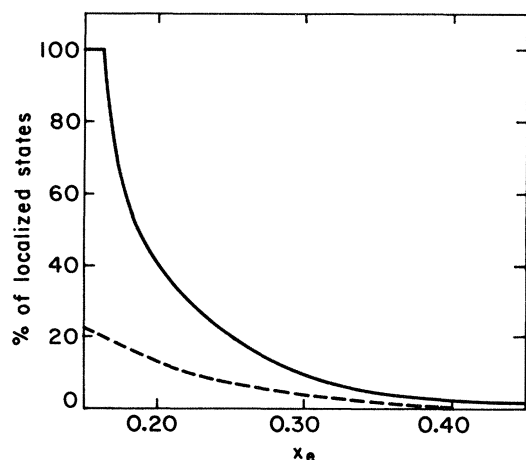
calized at pairs of atoms. At still smaller values of x_e additional pseudogaps form, and finally at $x_e \approx 0.16$ all of the states become localized. Thus $x_e \approx 0.16$ is the critical concentration for quantum percolation for states throughout most of the band. As usual the critical concentration for quantum percolation is higher than that for classical percolation.[11] At this point the density of states is similar to Fig. 2(a) of Jonson and Franz.[8] Thus it can be seen that as the mean coordination is reduced, the disorder in the system causes the energy band to split into subbands separated by pseudogaps.

The percentage of band states that are localized is shown as a function of x_e in Fig. 2. Also shown is the percentage of isolated atoms (those with no nearest neighbors) predicted by a random distribution. It is important to note that the percentage of isolated atoms is always much smaller than the percentage of localized states. In particular, the formation of most of the localized states in the center of the band is in no way dependent on the presence of isolated atoms, but instead depends on the number of atoms that have only a small number of neighbors.[23]

In Fig. 3 the two-site conductivity $\sigma_0(\epsilon)$ is shown as a function of energy for energies near the center of the band and for a range of x_e values. $\sigma_0(\epsilon)$ decreases rapidly as the mean coordination number decreases, as expected. At values of $x_e > 0.45$, $\sigma_0(\epsilon)$ is almost independent of energy throughout this central band region, while for
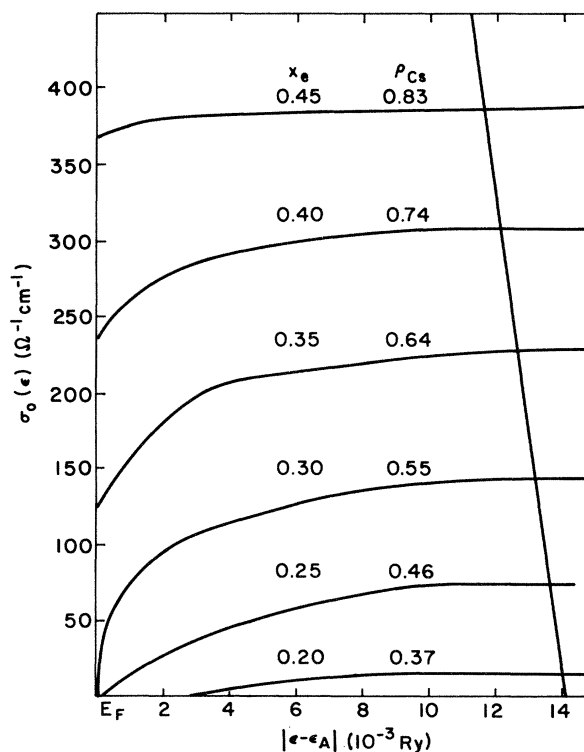

FIG. 2. Percentage of states that are localized as a function of the effective alkali-metal atomic concentration x_e. Solid curve: all localized states. Dashed curve: states localized on isolated alkali-metal atoms.

FIG. 3. Two-site conductivity $\sigma_0(\epsilon)$ as a function of energy for various values of the effective alkali-metal atomic concentration x_e. Also shown are equivalent values of the density ρ_{Cs} for expanded fluid Cs. Slanted line indicates for each x_e the approximate kT value at which experiments in expanded fluid Cs were performed.

$x_e = 0.30 \pm 0.1$ the energy dependence is very strong. At $x_e \cong 0.30$ the conductivity at the center of the band (at E_F) drops to zero. For smaller values of x_e, $\sigma_0(\epsilon)$ is zero over an ever-increasing range of energies until all of the states localize. It is interesting to note that for $x_e \lesssim 0.60$, the Kubo-Greenwood formula $\sigma(\epsilon) \propto [g(\epsilon)]^2$, is no longer applicable. Although there is a peak in $g(E)$ near the center of the band, the states within this peak have a lower mobility and thus do not contribute significantly to the conductivity, which is actually somewhat reduced in this region.

To calculate the conductivity $\sigma_0(0)$ it is necessary to carry out the integration indicated in Eq. (8). Rather than perform the integral numerically, we approximated it by averaging $\sigma_0(\epsilon)$ over the energy range $E_F - kT < \epsilon > E_F + kT$. The slanted line running through the curves in Fig. 3 indicates the approximate value fo kT, for each x_e, at which high-temperature ($T \sim 2000$ K) measurements for expanded Cs were made. Values of $\sigma_0(0)$ calculated from the curves in Fig. 3, using the indicated values of kT, are shown by the curve labeled "high T" in Fig. 5(a).

For the low-temperature alkali-metal—rare-gas film experiments, the values of kT are so much lower that the curves in Fig. 3 must be viewed with a greatly expanded energy scale. This is shown in Fig. 4 for alkali concentrations near 0.30. On this magnified energy scale the curves remain rather flat as the alkali-metal atomic concentration is decreased until $x_e \cong 0.30$. At this value of x_e we see a very rapid shift in the value of σ_0 ($\epsilon = \epsilon_A$). From our calculations, it appears that the change is discontinuous, opening up the possibility of a first-order phase transition at $x_e \cong 0.30$ or at a mean coordination number of ~ 3. From the error bars shown on the graph, however, it can be seen that large fluctuations occur in our numerical cal-

culations exactly in this region. It would be necessary to increase considerably the ensemble size and the number of iterations performed in order to investigate this further. The vertical line in Fig. 4 shows the value of kT for $T = 5$ K, a typical experimental temperature. The values $\sigma_0(0)$ calculated by averaging $\sigma_0(\epsilon)$ over this energy range are shown by the solid curve marked "low T" in Fig. 5(a). Also shown in Fig. 5(a) is a low-temperature curve with $Z_{max} = 10$ rather than the usual $Z_{max} = 9$. It can be seen from the curves of $\log \sigma_0$ vs x_e in Fig. 5(a) that for values of $x_e \lesssim 0.32$ the conductivity falls off much more rapidly with decreasing alkali-metal atomic concentration in the low-temperature regime than in the high-temperature regime.
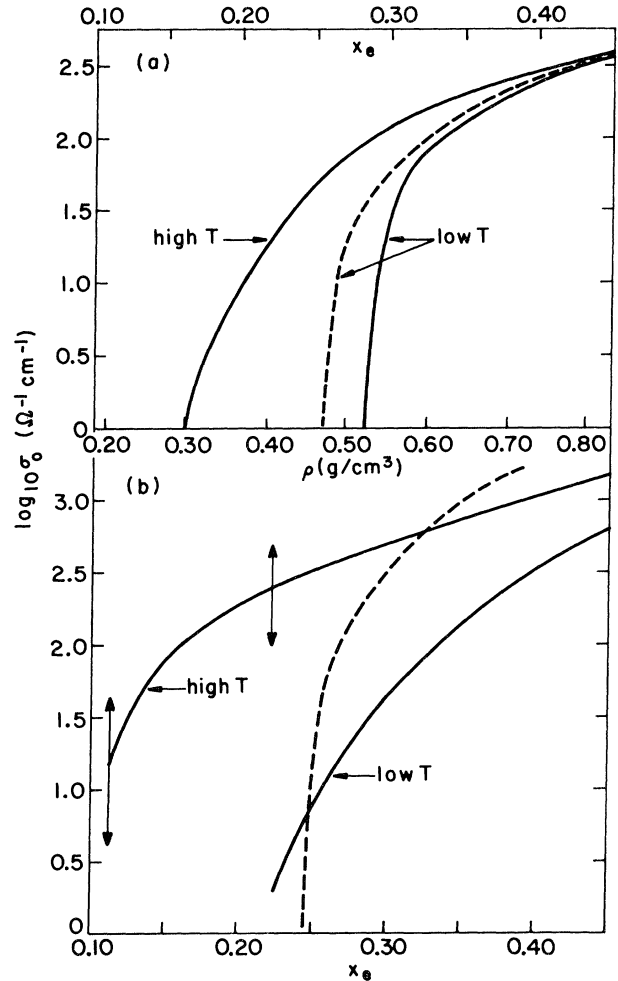
FIG. 5. Logarithm of the conductivity as a function of effective alkali-metal atomic concentration x_e. Scales for all curves are the same. An equivalent density scale, which is relevant only for the high-temperature measurements, is also given. (a) Calculated values of the two-site conductivity for the high-temperature regime, $Z_{max} = 9$, and for the low-temperature regimes, the solid curve is for $Z_{max} = 9$ and the dashed curve is for $Z_{max} = 10$. (b) Experimentally measured values of the conductivity. High-T curve is taken from the work on expanded fluid Cs by Franz et al. (Ref. 2). The low-T curves are taken from work on Cs-Xe; the solid curve is taken from Swenumson et al. (Ref. 16) and the dashed curve is taken from Phelps and Flynn (Ref. 6).
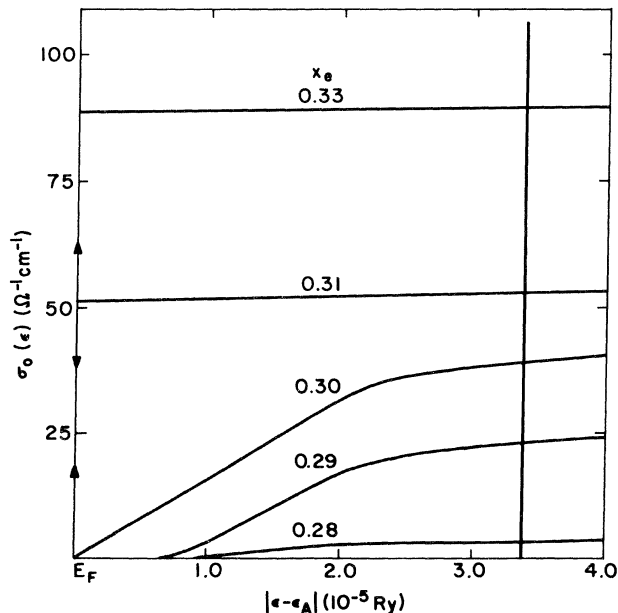

FIG. 4. Same as Fig. 3 but with an expanded energy scale. Vertical line indicates kT for 5 K, a typical experimental temperature. Note large uncertainties in the calculated results at $\epsilon = \epsilon_A$.

From the slopes of the curves in Figs. 3 and 4 it is possible to predict the qualitative temperature dependence of the conductivity $d \ln\sigma/dT$ as a function of x_e for the two temperature regimes. For the expanded alkali metals with $T \sim 2000$ K, as the effective alkali-metal atomic concentration is lowered, $d \ln\sigma/dT$ should become positive at $x_e \sim 0.45$ where a dip in the conductivity begins to form in the center of the band. It then increases continually until at $x_e \sim 0.25$, $d \ln\sigma/dT \geq 10^{-4}$/K. For the alkali-metal—rare-gas films with $T \sim 5$ K, the temperature dependence becomes positive at $x_e \sim 0.50$ and in this case it increases more rapidly as x_e is lowered. This is caused both by the larger values of $d\sigma_0(\epsilon)/d\epsilon$ and also by the smaller values of σ_0. For $x_e \sim 0.35$, one finds $d \ln\sigma/dT \sim 5 \times 10^{-4}$/K. As x_e is decreased further, the temperature dependence increases very rapidly and, as can be estimated from Fig. 4, at $x_e \sim 0.30$, $d \ln\sigma/dT \gtrsim 5 \times 10^{-2}$/K.

V. DISCUSSION

A. Expanded Cs

Among the alkali metals more experimental work has been carried out on Cs than the others because of its lower critical temperature and pressure. The measurements of Franz et al.[2] are given by the curve labeled "high T" in Fig. 5(b). Comparing these to our calculated values shown in Fig. 5(a), one can see that the two are in qualitative agreement $0.25 \lesssim x_e \lesssim 0.45$. Below this region, however, the two diverge with a low level of conduction actually persisting well beyond the point at which in our model all of the electrons are localized. We can suggest two possible contributions to this persistent conduction. The first comes from the motion of the atoms. Since the electrons are only well localized on a time scale $\tau \lesssim 10^{-13}$ sec, it is possible that thermal effects allow weak conduction to take place. The second contribution comes from the possible existence of free electrons. Freyland[17] has pointed out that a large fraction of Cs_2 molecules exist in this density region, and that their degree of ionization may be quite high due to a reduction in the ionization potential at high densities.[25]

As discussed in Sec. IV our model predicts a positive temperature dependence for the conductivity for values of $x_e \lesssim 0.45$, corresponding to $\rho \sim \rho_m/2 \sim 2\rho_c$. This is in excellent agreement with the experimental results.[2] We also predict that the temperature dependence increases as the density is lowered, with $d \ln\sigma/dT \geq 10^{-4}$/K at $x_e \sim 0.25$, but it has not yet been possible to measure the temperature dependence in this region. Of course, if the low-density conductivity is dominated by free electrons, as discussed above, the temperature dependence will be somewhat different in this region.

Measurement of the magnetic susceptibility along the liquid-vapor equilibrium curve for expanded Cs have been reported by Freyland.[17] From his plot of the gram susceptibility χ_g versus density, it can be seen that a large peak in the susceptibility occurs at densities very close to $\rho \sim 2\rho_c$. One explanation for the peak in the susceptibility is that it is caused by electron correlation effects that are

expected to be large in the neighborhood of a Mott-Hubbard transition. The susceptibility enhancement due to correlation effects has been calculated by Brinkman and Rice[26] and by Rose.[4] Rose predicted that the susceptibility enhancement should have a large peak at ρ_c rather than $\sim 2\rho_c$ where it is found experimentally. It is thus interesting to see how the susceptibility peak can be understood within the context of the model described in this paper.

Freyland[17] has calculated that the paramagnetic contribution to the gram susceptibility χ_g^p increases from a value of 0.6×10^{-6} cm^3/g, at a density of 1.5 g/cm^3, to a value of 1.3×10^{-6} cm^3/g at a density of 0.8 g/cm^3, and thus there is an increase in χ_g^p by a factor of 2.3. A major part of this increase is easily understood within the tight-binding framework. Lowering the density, and thus the mean coordination number, causes the Cs bandwidth to narrow and thus $g(E_F)$/atom increases as discussed in Sec. IV. This effect can be seen from the curves in Fig. 1. Because $\chi_g^p \propto \bar{g}(E_F)$/atom [where the overbar indicates that $g(E_F)$ is averaged over the states within $\sim kT$ of the Fermi surface], it must also increase. The tight-binding model yields $g(E_F)$/atom $\propto 1/\bar{Z}$, so that it predicts the following increase in susceptibility for the above-mentioned density interval:

$$\frac{\chi_g^p(0.8 \text{ g/cm}^3)}{\chi_g^p(1.5 \text{ g/cm}^3)} = \frac{\bar{Z}(1.5 \text{ g/cm}^3)}{\bar{Z}(0.8 \text{ g/cm}^3)} = 1.9 .$$

[Note that our calculations are done on a Cayley-tree lattice for which the relationship between $g(E_F)$/atom and $\bar{Z}$ is slightly different from the usual tight-binding model.[22] Thus the enhancement in $g(E_F)$/atom shown in Fig. 1 is slightly less than 1.9.] Thus only a small part of the measured enhancement needs further explanation. Another way of viewing this is to note that the volume susceptibility χ_V^p should be independent of $\bar{Z}$ in the tight-binding model. Plots of the measured χ_g^p versus density show that a peak still remains, but that it is now greatly reduced in size.

We think that the remaining peak in χ_V^p can be understood in terms of the piling up of states near the Fermi energy that, as can be seen from the curves in Fig. 1, begins at $x_e \sim 0.6$ or at $\rho \sim 1.1$ g/cm^3. These additional states do not contribute significantly to the conductivity (see Fig. 3), and it is probable that they are weakly localized. However, we would expect these states to contribute fully to the susceptibility. The number of weakly localized states with a range $\sim kT$ of the Fermi energy appears to peak around $x_e \sim 0.45$ or $\rho \sim 0.8$ (see Fig. 1). For lower densities the spike of highly localized states at E_F grows very rapidly, while other states are excluded from this energy region. Freyland's measurements[17] lead us to believe that these highly localized states contribute only weakly to the susceptibility. Since the majority of the localized states are not localized on isolated atoms, it is reasonable that their magnetic properties appear to be more molecular than atomic.

B. Comparison of expanded alkali metals

It is interesting to consider what general insights about alkali metals at low densities can be obtained from our

model. We restrict our discussion to low densities, $\rho \lesssim \rho_m/2$, because the inherent approximations of our tight-binding model make it inappropriate for discussion of alkali-metal systems at densities where they are good metals.

Because the model contains only two parameters, it is straightforward to use it to predict the relation of the properties of different alkali metals. The value of the coordination number at the melting point, $Z_{max}=9$, was taken from experiments on Rb,[3] but it is a reasonable number for liquid metals in general. Once Z_{max} is fixed, the value of the hopping integral t is set by the bandwidth of the metal at the melting point. In the tight-binding model the bandwidth is given by $2Z_{max}t$, so that the Fermi energy of a half-filled band is related to t by $E_F=Z_{max}t$. Since the value of E_F varies by a factor of 2 between Na and Cs, the appropriate t value for Na would be about twice that used in our calculations. Changing t changes the absolute energy scales in Figs. 1, 3, and 4, while leaving the shapes of the curves unchanged. Thus as one moves up the Periodic Table from Cs, and the Fermi energy and bandwidth of the alkali metals increase, the shapes of the density-of-states curves as a function of x_e remain the same; the localized states still appear at identical values of reduced density ρ/ρ_m as before. Moreover, the values of $\sigma_0(E)$ near the Fermi surface remain essentially the same because, as shown by Eq. (7), the expression for $\sigma_0(E)$ contains a factor of t^2 that cancels the effect of each factor of $1/t$ in the density of states (proportional to ImG_{ii}). However, the conductivity is given by the integral in Eq. (8) and is thus an average of $\sigma(\epsilon)$ over a range of $\sim 2kT$ near the Fermi energy. This range will cover a smaller percentage of the total band as t increases; thus for constant T, the conductivity will decrease somewhat as t increases. This change in σ will be negligible, however, for $\rho \gtrsim \rho_m/3$, because the $\sigma(\epsilon)$ curves are relatively flat in this region. Thus the model predicts that the conductivities of the alkali metals at low densities should be very similar to each other as a function of reduced density ρ/ρ_m, the conductivity of the lighter alkali metals being somewhat less than those of the heavier for values of ρ approaching the critical density ρ_c. Experiments by Franz et al.[2] have shown the conductivities of Rb and Cs are indeed very similar function of ρ/ρ_m. Many other properties of the alkali-metals, including the paramagnetic contribution to the magnetic susceptibility and the Knight shift, should also scale as a function of ρ/ρ_m.

Our model indicates that the metal-nonmetal transition takes place gradually, with extended states and localized states existing together over a wide range of densities. Thus the location of the transition depends on how it is defined. If the transition is defined by the temperature dependence of the conductivity, i.e., the density at which the temperature dependence of the conductivity changes from negative to positive, then the transition should occur at values of $\rho/\rho_m \sim 0.45$ for all of the alkali metals. On the other hand, using the usual definition of the metal-nonmetal transition, that it occurs at the minimum density for which $\sigma \not\to 0$ as $T \to 0$, one finds the transition at $\rho/\rho_m \sim 0.30$ for all of the alkali metals.

The model presented in this paper also yields insight

into the nature of the critical point in the alkali metals. The major contribution to the cohesive energy in liquid alkali metals at normal densities comes from the metallic binding which depends on the bandwidth. As the density of the liquid is reduced below its value at the melting point, the bandwidth narrows (see Fig. 1) and the cohesive energy is reduced. This is a slow and continuous process. As the density is reduced below $\sim \rho_m/2$, however, something more dramatic happens: localized states appear and most of these pile up at the Fermi energy. Electrons at the Fermi energy do not make any positive contribution to the metallic binding. The metallic contribution to the cohesive energy thus falls as the percent of localized states rises. This is quite rapid below $x_e \sim 0.30$ (see Fig. 2). The remaining van der Waals interaction is, however, insufficient to bind large clusters of atoms at the high temperatures involved, so the disappearance of the metallic binding leads to a critical point. Within this model ρ_c/ρ_m should be approximately the same for all the alkali metals. It is interesting to note that the value of ρ_c/ρ_m for Cs, Rb, and K are all $\rho_c/\rho_m=0.23\pm0.005$.[3] At this value $\sim 25\%$ of the band states are localized. The model developed in this paper thus offers a simple description of the nature of the critical point in alkali metals and may be valid for other simple metals as well.

C. Alkali-metal—rare-gas films

In the low-temperature regime changes in the physical properties of dilute alkali-metal systems can be observed without the thermal smearing that occurs at high temperatures. Changes that occur as a function of concentration are thus expected to be sharper. This sharpening of the metal-nonmetal transition is predicted by our model and can be seen from the results shown in Fig. 5(a).

The validity of our model for dilute alkali-metal systems can be checked by comparing it to experimental results for alkali-metal—rare-gas films. As discussed in the Introduction, the analysis of these results is greatly simplified by making the customary assumption that the rare-gas atoms are totally inert and act only as holes in the alkali metals. At a sufficiently low alkali-metal atomic concentration this assumption must break down because it is well known that Cs-Xe molecules are stable at very low temperatures and pressures.[27] It would be possible to include a weak Cs-Xe interaction in our calculations, but up until now we have not done so.

Experimental measurements have been carried out in Cs-Xe,[16] Rb-Kr,[6] and Na-Ar (Ref. 13) films. Each of these systems has been found to have a metal-insulator transition that occurs over a rather narrow range of concentrations. For Cs-Xe and Rb-Kr this rapid decrease in conductivity occurs at an alkali-metal atomic concentration ~ 25 at. % while for Na-Ar the value is ~ 55 at. %. It is necessary, therefore, for our model to be able to account for these transitions with the two parameters Z_{max} and t. We consider first the effect of Z_{max}.

There are no direct experimental measurements to guide the selection of Z_{max}, the maximum number of nearest neighbors surrounding an alkali metal atom. Although $Z_{max}=9$ is a reasonable value for a pure liquid or amor-

phous metal in which all the atoms are the same size, one expects that for alloys it will vary somewhat with the relative atomic size of the constituents. At low alkali-metal atomic concentrations, it is expected that $Z_{max} > 9$ if the rare-gas atoms are smaller than the alkali-metal atoms and $Z_{max} < 9$ in the reverse case. Our model predicts that the conductivity increases with increasing Z_{max} since a large Z_{max} implies that a large number of paths are available for electron hopping. This can be seen from our calculated results shown in Fig. 5(a), where the conductivity as a function of alkali-metal atomic concentration is plotted for both $Z_{max} = 9$ and 10. Z_{max} can also be expected to vary somewhat with alkali-metal atomic concentration, but this will have little or no effect over the narrow concentration range where the metal-insulator transition occurs.

The two sets of experimental measurements on Cs-Xe shown in Fig. 5(b) are not in close agreement with each other.[28] Our calculated curve with $Z_{max} = 10$ is in good qualitative agreement with both measurements although a value of $Z_{max} = 11$ would probably agree somewhat better with the results of Swenumson et al.[16] Since the Xe atoms are slightly smaller than the Cs atoms, values of 10 or 11 are quite reasonable. The conductivity as a function of concentration in Rb-Kr is very similar to that in Cs-Xe.[6] This would be expected in our model since the atomic radii have very nearly the same ratio, so that Z_{max} should be the same for both systems, and any differences between the two would be due to the small difference in t. The effect of changing t was discussed in Sec. V B where it was shown that $t = E_F/Z_{max}$. Thus for fixed Z_{max}, $t_{Rb}/t_{Cs} \sim 1.2$. The only effect of changing t by 20% is to sharpen the metal-insulator transition slightly. Thus the close similarity between Cs-Xe and Rb-Kr can be understood within our model.

The other alkali-metal—rare-gas system, Na-Ar, for which recent measurements exist has been found to have a metal-insulator transition at ~ 55 at. % Na. Since Ar atoms are larger than Na atoms, our model suggests a value of $Z_{max} < 9$. From a few preliminary calculations, we find that the rapid change in σ_0 at a concentration of ~ 55 at. % can be reproduced using a $Z_{max} \sim 5.5$, a reasonable value. It appears that our model does a good job of describing the metal-insulator transitions observed in dilute alkali-metal systems at low temperature. Moreover, in contrast to classical percolation, this calculational technique can be used to study other properties of these systems as those described below.

Because the alkali-metal—rare-gas films are found to be unstable as the temperature is increased above 5—10 K, few temperature-dependent measurements have been performed. Swenumson et al.[16] report that the conductivity has a positive temperature dependence in the range $0.22 > x_{Cs} > 0.51$, in excellent agreement with the predictions of our model as discussed in Sec. IV. Moreover, they found that in this concentration range $d \ln\sigma/dT \sim 10^{-2}/K$. Although we would expect the value to be somewhat smaller than this for $x_{Cs} > 0.35$, our calculations indicate that the temperature dependence increases rapidly for lower concentrations, reaching a value of $\sim 5 \times 10^{-2}/K$ for $x_{Cs} \sim 0.30$. Thus the sign and the

rough order of magnitude of the observed temperature can be well explained by our model.

Our model also provides insight into the observed thermal instability of the alkali-metal—rare-gas films.[16] In Sec. V B we discussed the change in the metallic contribution to the cohesive energy as a function of alkali-metal atomic concentration. We indicated that our model predicts a rapid decrease in the metallic binding below $x_{Cs} \sim 0.45$ caused by a rapid growth in the spike of localized states at E_F. Thus at low alkali-metal atomic concentrations, random films would be held together predominantly by the van der Waals interaction. Under those conditions it becomes energetically favorable for the alkali-metal atoms to cluster to regain metallic binding, making it difficult to maintain random films. This can be contrasted with other alloys in which charge transfer occurs. These have an ionic contribution to the binding which provides increased stability throughout a wide concentration range.

Swenumson et al.[16] have indicated that their investigation of the optical properties of Cs-Xe films shows that a metal-insulator transition takes place at $x_{Cs} = 0.55 \pm 0.01$. As for the expanded alkali metals, our model indicates that the exact location of this transition in Cs-Xe films is a matter of definition since both extended and localized states exist over a wide range of concentrations. Our calculations indicate, however, that $d\sigma(\epsilon)/d\epsilon \mid_{E_F}$ becomes positive at $x_{Cs} \sim 0.5$ (leading to the positive temperature dependence for σ), and it may be that it is this change that the optical properties are displaying. We have not attempted to predict optical properties on the basis of our model.

In light of the recent discussion on "minimum metallic conductivity"[29] it is interesting to ask what our model predicts for the $T \rightarrow 0$ behavior of the conductivity. Calculations performed so far appear to favor a small jump in the $T = 0$ conductivity (see Fig. 4) and a minimum metallic conductivity σ_{min} of ~ 50 $\Omega^{-1}cm^{-1}$, although the scatter in our numerical calculations near $x_e \sim 0.30$ is very large as we have indicated with error bars. Using Mott's equation,

$$\sigma_{min} = 0.026 e^2/\hbar a ,$$

one finds, for Cs, a value $\sigma_{min}^{Cs} \sim 100$ $\Omega^{-1}cm^{-1}$, which is within a factor of 2 of our preliminary result. More extensive calculations are currently underway to test the idea of σ_{min} within this model. If we find that the conductivity falls smoothly to zero with x_e, this will be an example of the possible exceptional systems that Mott[29] describes for which $\sigma < \sigma_{min}$ only in a very narrow range of concentration.

VI. CONCLUSIONS

Using a simple tight-binding model that incorporates realistic atomic-scale disorder in dilute alkali-metal systems, we have been able to obtain results that are in good qualitative agreement with a wide range of experimental measurements for both expanded alkali metals and alkali-metal—rare-gas films. Although electron correlation effects may play a role in the metal-insulator transitions in

these materials, our calculations indicate that disorder is probably a dominant factor.

The model's simplicity makes it a valuable tool for studying scaling relations and critical phenomena in alkali-metal systems as we have indicated by our initial work discussed in this paper. In addition, it seems probable that the model will prove to be applicable to a broader range of systems than just those containing alkali metals. We plan to use the ideas developed in this paper to investigate a variety of other systems.

ACKNOWLEDGMENTS

[1]N. F. Mott and E. A. Davis, *Electronic Processes in Noncrystalline Materials* (Clarendon, Oxford, 1979).

[2]G. Franz, W. Freyland, and F. Hensel, J. Phys. (Paris) Colloq. 8, C-70 (1980).

[3]W. Freyland, Comm. Solid State Phys. 10, 1 (1981).

[4]J. H. Rose, Phys. Rev. B 23, 552 (1981).

[5]P. W. Anderson, Phys. Rev. 109, 1492 (1958).

[6]D. J. Phelps and C. P. Flynn, Phys. Rev. B 14, 5279 (1976).

[7]S. Kirkpatrick and T. P. Eggarter, Phys. Rev. B 6, 3598 (1972).

[8]M. Jonson and J. R. Franz, J. Phys. C 13, 5957 (1980).

[9]Y. Shapir, A. Aharony, and A. B. Harris, Phys. Rev. Lett. 49, 486 (1982).

[10]A. B. Harris, Phys. Rev. Lett. 49, 296 (1982).

[11]R. Raghavan and D. C. Mattis, Phys. Rev. B 23, 4791 (1981).

[12]S. N. Evangelou, Phys. Rev. B 27, 1397 (1983).

[13]N. A. McNeal and A. M. Goldman, Phys. Lett. 61A, 268 (1977).

[14]D. Adler, L. P. Flora, and S. D. Sentaria, Solid State Commun. 12, 9 (1973).

[15]H. Scher and R. Zallen, J. Chem. Phys. 53, 3759 (1970).

[16]R. D. Swenumson, S. Leutwyler, and U. Even, Phys. Rev. B 24, 5726 (1981).

[17]W. Freyland, Phys. Rev. B 20, 5104 (1979).

[18]R. Abou-Chacra, P. W. Anderson, and D. J. Thouless, J. Phys. C 6, 1734 (1973).

[19]W. Freyland, F. Hensel, and W. Gläser, Ber. Bunsenges. Phys. Chem. 83, 884 (1979).

[20]K. M. Watson, Phys. Rev. 105, 1388 (1957).

[21]F. Brouers, M. Cyrot, and F. Cyrot-Lackmann, Phys. Rev. B 7, 4370 (1973).

[22]J. R. Franz, F. Brouers, and C. Holzhey, J. Phys. F 10, 235 (1980).

[23]J. R. Franz and J. H. Rose (unpublished).

[24]M. Jonson and S. M. Girvin, Phys. Rev. Lett. 43, 1447 (1979).

[25]F. Hensel, Habilitationsschrift, University of Karlsruhe, 1970.

[26]W. F. Brinkman and T. M. Rice, Phys. Rev. B 2, 4302 (1970).

[27]G. D. Mahan and M. Lapp, Phys. Rev. 179, 19 (1969).

[28]For a discussion of the differences between the two measurements, see, R. Avci and C. P. Flynn, Phys. Rev. B 27, 3886 (1983).

[29]N. F. Mott, Philos. Mag. B 44, 265 (1981).